
Article:
Ingham Dempster, T., Corfe, B.M. and Walker, D.C. (2018) A cellular based model of the colon crypt suggests novel effects forApc phenotype in colorectal carcinogenesis. Journal of Computational Science, 24. pp. 125-131. ISSN 1877-7503

https://doi.org/10.1016/j.jocs.2017.06.013

A Cellular Based Model of the Colon Crypt Suggests Novel Effects for Apc Phenotype in Colorectal Carcinogenesis

Tim Ingham-Dempster[1,2,*], Dr Bernard Corfe[1,2], Dr Dawn Walker[1,3]

1 INSIGNEO Institute, University of Sheffield, England
2 Molecular Gastroenterology Research Group, Department of Oncology and Metabolism, University of Sheffield, England
3 Department of Computer Science, University of Sheffield, England

* Correspondence: taingham-dempster1@sheffield.ac.uk, Tim Ingham-Dempster, The Medical School, The University of Sheffield, Beech Hill Road, Sheffield, S10 2RX

1. Abstract

Colorectal cancer (CRC) is a major cause of cancer mortality; loss of the Apc gene is an early step in the formation of CRC.

A new computational model of the colonic crypt has been developed to simulate the effects of Apc loss. The model includes a region of flat mucosa, which has not previously been considered in the context of Apc loss.

The model suggests that Apc loss confers a survival advantage at the crypt mouth which may be a previously unknown method of mutation fixation.

2. Introduction

2.1 Biological Background

The human large intestine consists of an epithelial monolayer forming the flat mucosal surface, punctuated by glands known as the crypts of Lieberkuhn (**Fig 1A**). These crypts are the functional unit of the colonic epithelium, supporting the rapid turnover of cells in the organ through constant division and differentiations of stem cells located at their base: as such the perturbation of their turnover and inappropriate accumulation of cells is implicated in formation of colorectal cancer (CRC) (1). Identifying these underlying homeostatic processes is therefore crucial in understanding the pathophysiology of colorectal disease.

A human colonic crypt contains approximately 2500 cells, or colonocytes (2). There is a stem cell compartment at the base of the crypt which is estimated to comprise around 10 cells (3) which are purple in **Fig 1A**. Cells exiting the stem cell compartment (variously called transit amplifying cells or proliferating cells, light blue in the figure) account for around 25% of cells in the crypt (4). Fully differentiated cells include water-absorbing colonocytes (red) which compose roughly 75% of differentiated cells, mucus secreting goblet (green) cells which account for roughly 24% of differentiated cells and hormone secreting enteroendocrine cells (yellow) which differentiate directly from stem cells rather than from transit amplifying cells and account for less than 1% of differentiated cells (2, 5).

Cell proliferation and differentiation along the crypt axis is governed by a gradient of Wnt3, being strongest at the bottom of the crypt where proliferation rates are highest (6). This proliferation is balanced by anoikis - a form of cell death occurring when a cell loses contact with the basement membrane (7). It is thought to occur at the top of the crypt where cells are shed into the intestinal lumen as a normal physiological process maintaining cellular homeostasis in the tissue (8). In normal tissue a constant cycle of cell proliferation and loss results in a homeostatic condition where the entire crypt (stem cells aside) is turned over every 4-7 days in humans (9).

Abnormalities in these cell replacement processes are strongly implicated as the earliest stages in CRC development. Loss of function of the tumour-suppressor protein Apc due to mutation is a known step in early carcinogenesis (1). The changes in cell properties due to Apc loss are characterised in-vitro but their overall effect on crypt dynamics is not well understood.

There are two main effects of Apc loss on epithelial cells. The first effect is upregulation of proliferation due to activation of the Wnt pathway. APC forms a destruction complex for β-catenin preventing it from accumulating in the nucleus where it upregulates proliferative genes. WNT3 acts by binding APC and preventing it from forming the beta-catenin destruction complex thus allowing beta-catenin to accumulate and migrate to the nucleus, loss of the Apc gene prevents the beta-catenin destruction complex from forming which allows beta-catenin to accumulate in the same manner as if the Wnt pathway were activated. This leads to cells proliferating in a similar manner to cells in a high WNT environment regardless of the actual level of WNT available (10).

β-catenin is also known to be vital for cell-cell adhesion (11) and this can also be regulated by Apc based destruction. Loss of Apc leads to more β-catenin being available to form cell adherens junctions and therefore stronger cell-cell adhesion. Adhesive interactions with the extra cellular matrix may affect the process of anoikis. An increase in adhesion with the extra cellular matrix may also lead to an increased amount of drag on passively migrating epithelial cells.

We hypothesise that these mechanical changes will result in mutated cells displaying different behaviour to wild-type cells, in particular at the crypt mouth.

2.2 Computational Modelling

The dynamic nature of the processes within the crypt means that they are impossible to study through traditional experimental methods. Biopsies and animal models can only provide snapshots of the crypt at a single moment in time and extrapolating from one timepoint to another is challenging due to the emergent nature of certain processes. Due to these difficulties, the crypt is an attractive target for computational methods. A range of computational models have been applied to crypt dynamics, which vary in terms of their basic assumptions, underlying methodologies, and degree of spatial resolution.

Compartment models (Tomlinson et al (12), Smallbone et al (13)) consider the composite behaviour of different populations of cells within the crypt and implement rules governing the growth and interactions between these populations in the form of ordinary differential equations (ODEs). The crypt has also been modelled as a continuum (14) using partial differential equations to represent the spatial distribution of the different cell compartments. In this context, cells are still modelled as populations rather than discrete entities. The first models to consider cells as individual entities were lattice based models - an approach still in use due to its computational efficiency (4). Here the crypt is modelled as a lattice, or grid, where each lattice point or node can be occupied by a cell. The limitation here is that cells can only move from space to space in discrete jumps meaning realistic intercellular interactions cannot be modelled. This limitation can be overcome by using a more complex modelling paradigm such as the Cellular Potts method, which was used to show that Ephrine signalling can cause cells to sort into spatially distinct regions within the crypt (15). However these models have the disadvantage of being computationaly expensive.

Agent-based models (ABMs) represent cells as free agents moving in space (16). Each cell acts as an independent agent with no globally overarching control. This approach is appealing for biological modelling as it captures the nature of biological cells as individual autonomous entities that can respond to signalling cues, and also allows the modeller to capture the important concept of intercellular heterogeneity (17).

In most existing models, cell death is not explicitly related to a biological mechanism, but attempts to capture phenomenologically the known behaviour that cells predominantly die at the top of the crypt. For instance, a deterministic cell death rule is activated as soon as a cell reaches the top of the crypt (16) or cells die stochastically with a probability that increases towards the crypt top (4).

Mirams et al (18) developed an agent based model to study the effects of Apc gene mutation on the crypt. Increased proliferation, a larger proliferative compartment for $Apc^{-/-}$ (i.e. both copies of the Apc gene have been mutated) cells and a stronger basement membrane attachment for $Apc^{-/-}$ cells were modelled and placed in competition with wild type cells within a crypt. Survival advantages were found for all three effects of Apc loss. The geometry of the crypt mouth was not modelled and cell death was modelled by a rule which removed any cell that reached the top of the crypt, as such it was impossible to model the interaction between Apc loss and Anoikis.

Dunn et al (19) used an agent based model to examine the role of the basement membrane in crypt formation and also included the concept of anoikis. The model predicted that whilst anoikis did occur at the crypt mouth, it also occurred throughout the crypt and was most prominent at the crypt base. As such, there was no significant cell migration in the simulated crypt and a phenomenological rule dictating cell death at the crypt mouth had to be introduced to give rise to the correct migration behaviour.

Previously we have developed an ABM to study homeostatic processes within the crypt (20). This model extended earlier work by explicitly modelling the crypt mouth for the first time and including rules to simulate anoikis. Unlike the only previous study (19) to include anoikis this model was able to correctly predict the localisation of anoikis to the crypt mouth by incorporating a more accurate model of the cell geometry. Another prediction of this model was that anoikis regulates cellularity within the crypt and is a key homeostatic process. As suggested by biological experiment (21), anoikis rates emergently matched proliferation rates and constrained the crypt to a steady state under all test conditions. Changes in proliferation rates did lead to changes in the steady state equilibrium point for cellularity which displayed non-linearities and we hypothesise that these processes may be sensitive to the effects of Apc mutation. We were motivated to study the crypt mouth in order to fulfil our longer term aim of developing a multi-crypt model including a representation of the flat mucosa between adjacent crypts.

It has been shown that mutations in a crypt cell can become permanently fixed in the crypt through a process called monoclonal conversion (**Fig 1B**). The influence of Apc loss on this process is not fully understood and the interaction of Apc loss, monoclonal conversion and anoikis has not previously been investigated.

We sought to extend our ABM (20) in order to explore the consequences of Apc loss on the crypt's homeostatic mechanisms. We added rules for mutated cells and code to track populations of such cells as described in section 3.

3. Materials and Methods

An agent based model was used to investigate the interaction of Apc mutation, monoclonal conversion, and anoikis. Unlike previous crypt models it explicitly includes a representation of anoikis and a realistic representation of the morphology of the crypt top. Details of this model are available in our previous paper (20) and a summary is presented below:

In the model each cell is represented by a software agent which behaves according to its own internal state and known biological signals, with no global control. Cells move in three dimensions due to a number of forces acting upon them. The main force is that of cell-cell repulsion which causes the majority of movement within the crypt. This is modelled as a pairwise damped spring system obeying **Eq. 1**.

$$\mathbf{F} = ((r_1 + r_2 - |\mathbf{p_1} - \mathbf{p_2}|) * ((\mathbf{p_1} - \mathbf{p_2}) / |\mathbf{p_1} - \mathbf{p_2}|) * k) \text{ iff } |\mathbf{p_1} - \mathbf{p_2}| < r_1 + r_2 \quad (1)$$

Where k is a constant determining the strength of the force, $\mathbf{p_1}$ and $\mathbf{p_2}$ are the locations of the two cells, and r_1 and r_2 are the radii of the two cells (**Fig 1C**). Neglecting inertial effects (i.e. assuming a dmaped spring model where momentum from the previous timestep can be ignored) the velocity of the cell is then determined solely from this force (16).

The agents progress through a simple cell cycle that incorporates quiescence, growth, and division depending on time and location within the crypt. This is based on the niche hypothesis (22) of cell function within the crypt and is driven by a simulated gradient of WNT3. The length of the growth phase (G1) for each cell is individually stochastically sampled from a normal distribution with mean and standard deviation taken from the literature (6), the timespan of the quiescent (G0) and division (M) phases are simple timespans which are identical across all cells and sourced in the same way as the value for growth phase.

An additional force represented using the damped spring model described by **Eq. 2** and of the same form as **Eq 1** acts to keep cells in contact with the basement membrane. In the event that cells are forced away from the membrane, anoikis is induced when a threshold separation is reached.

$$\mathbf{F} = (\mathbf{p_1} - \mathbf{p_b}) * k_b \quad (2)$$

Where k_b is the parameter controlling the strength of attachment to the basement membrane, $\mathbf{p_1}$ is the location of the cell, and $\mathbf{p_b}$ is the location of the closest point on the membrane to $\mathbf{p_1}$ (**Fig 1C**).

The existing model was extended to allow mutated cells to be included, and particular properties (quiescent time, membrane attachment strength, and cell drag) varied depending on whether cell agents have those properties tagged as mutated or wldtype. Mutated properties are inherited by daughter cells following cell division.

The model results in a three-dimensional simulation of the crypt where cells originate in a small stem cell compartment at the bottom of the crypt and flow up to the flat mucosa, undergoing a period of rapid proliferation. Our previous paper showed the existing model is in good agreement with other models of the crypt and displays phenomena such as monoclonal conversion and passive migration of cells (16, 20, 22-25).

A number of in-silico experiments were undertaken using this model. In each case the simulation was run for a thousand timesteps, with each timestep corresponding to 30 seconds of biological time, to achieve a stable homeostatic condition before a single randomly selected cell near the crypt base was “mutated”, as described in the previous paragraph. The size and spatial locations of the population of mutated cells was then

tracked through the rest of the simulation. Total simulation time was equivalent to ~1 year of biological time. Each simulation was repeated ten times to account for stochasticity due to cell cycle times being sampled from a normal distribution to reflect biological reality.

Parameter values for the experiments were identical to those used in our previous paper (20), where a number of parameters were tested including mean cell cycle time and the attachment force parameter. In that study, the median values of a 30 hour mean cell cycle time and a 0.001 (unitless) attachment force were used.

Here, we describe five virtual experiments assessing the impact of different aspects of Apc mutation on the crypt.

Experiment 1 studies the behaviour of a wild-type clonal population originating from a single cell with no mutation effects to provide a baseline for comparison.

Experiment 2 investigates the effects of increased adhesion of Apc mutated cells to the basement membrane. To do this the adhesion parameter of a single cell was increased ten-fold and this new value was inherited by any daughter cells upon division. The clonal population arising from this cell was then tracked throughout the simulation.

Experiment 3 examines the effects of increased cell drag from the basement membrane on Apc mutated cells. This was achieved by halving the velocity arising from the repulsive force between cells at each timestep for any cell in the clonal population of the original mutated cell, again this clonal population was tracked throughout the simulation.

Experiment 4 looked at the effect of reducing the quiescent time of stem cells in Apc mutation. In this experiment the initial mutant cell had its quiescent time reduced to 10%. Again the clonal population generated by this cell was tracked throughout the simulation.

Experiment 5 combined the three previously studied effects by modifying a single cell to have all three mutation effects and tracking its clonal offspring throughout the simulation.

4. Results

4.1 General properties and behaviours of a clonal population in the model crypt

The first experiment created a "neutral" mutation which could be tracked but did not confer any changes to the properties of the mutated cells. This was used as a baseline to determine the expected cell counts for a clonal population arising from a single cell.

An example of the crypt with this mutation is shown in **Figure 2Ai**. Red cells are wild-type and black cells are mutated. Small groups of neutrally mutated cells emerge from the stem cell niche and enter the proliferating compartment where they expand into small streams of cells in the expected ribbon pattern seen in biological experiments (26). This ribbon occurs as cells are being produced rapidly in an environment containing a directed flow, this is somewhat analogous to injecting smoke into a moving airflow. The clonal population dies out over time due to the phenomenon of monoclonal conversion which has been thoroughly examined in previous studies (18, 24).

Figure 2Aii shows the number of neutrally mutated stem cells in the crypt and in the flat mucosa with **Fig 2Aiii** showing the percentages of crypt and flat mucosal cells which are neutrally mutated. From these data, it can be seen that a small clonal population arises in the crypt and persists for a period of time before dying out. It is also evident that the population in the flat mucosa lags that of the crypt population as expected from the fact that cells arise in the crypt and then migrate to the mucosa. Error bars give a baseline for the variance due to simulation stochasticity of a clonal population of wild type cells in the crypt allowing comparisons to be drawn with mutated cells in later simulations. Finally the neutral mutation did not approach crypt dominance in any of the simulations (**Table 1**), suggesting that this cell location cannot give rise to a dominant population without some change conferring an advantage in niche succession.

4.2 Individual and cumulative effects of Apc-loss phenotype

The second simulation series created a mutation which increased the mutated cells' adhesion to the basement membrane of the crypt. **Fig 2Bi** shows a snapshot of the simulation with this mutation. From this image (which is typical of the series) it can be seen that mutated cells are the majority of cells in the flat mucosa and also form small clusters whilst in the crypt.

Fig 2Bii shows counts of mutated cells in the crypt and in the flat mucosa over time and **Fig 2Biii** shows the percentage of crypt cells which are mutated in green and the percentage of mutated mucosal cells in blue. Both figures show that the flat mucosa supports a much larger population of mutated cells than in the case of neutral mutation which suggests that an increase in basement attachment confers a major advantage to cells in the flat mucosa.

Figs 2Bii and **iii** also show that there was a small increase in the counts and percentages of mutated cells in the crypt compared to the neutral mutation, along with an increased variance. The raw data shows a single simulation run with approximately 50% mutated cells at the end and the mutated line being extinct in the other nine runs, additionally the mean time to mutant population extinction was longer in the other nine runs than in the simulations with a neutral mutation (**Table 1**).

A set of simulations were run where mutated cells were assigned a reduced cell-cell repulsion force to simulate the additional drag caused by increased membrane adhesion. A visualisation of a typical crypt from this run can be seen in **Fig. 2Ci.** This visualisation shows that cells with this mutation tend to form a small number of large clusters instead of many small groups, as was observed in the case of non-mutated cells.

Figure 2Cii shows the counts of mutated cells in the crypt and flat mucosa, **Fig 2Ciii** shows this data as percentages of cells mutated. These data show that crypt mutated cell counts are larger than for the neutral mutation, equating to a major survival advantage in the crypt. The graphs also show a very large standard deviation across these simulations. This can be explained by the fact that three of the ten crypt simulations resulted in predictions that the crypt would be 100% mutated by the end point whereas in the other seven runs the mutated population became extinct (**Table 1**). Additionally the mutated crypts had twice the cell count of the wild-type crypts.

The increases in mutated cell counts / percentages and variance can also be seen in the flat mucosa. These populations track the crypt population with a time lag as seen for the mutated populations in the neutral mutation experiments.

The fourth experiment investigated the effect of reducing the duration of the quiescent period in mutated stem cells, which is also believed to be an effect of Apc mutation [2]. **Fig. 2Di** is a snapshot taken from a crypt during this simulation. As can be seen a large continuous ribbon of mutated cells stretches from the niche to the crypt mouth, a phenomenon also observed in-vivo (26).

Figs 2Dii and **2Diii** show mutated stem counts and proportion of cells mutated for both crypt and flat mucosa. This shows that in all simulations the crypt became 100% mutated after approximately 50 days (**Table 1**). There was a larger variability than the neutral mutation during the mutant population expansion phase. These data clearly show that quiescence reduction confers a major advantage in the stem cell niche.

A large increase in the percentage of mutated cells within the flat mucosa is also apparent. This expansion within the flat mucosa followed expansion within the crypt in a similar manner to the neutral mutation. The mutated population did not occupy more than 70% of the flat mucosa despite the crypt supplying a constant stream of mutated cells into the mucosa.

The final set of simulations combined the three effects previously examined individually to represent the range of known effects of Apc loss. A visualisation of a typical crypt with this mutation can be seen in **Figure 2Ei.** This shows all three effects in evidence: the niche has been colonised by mutant cells which form a very dense cluster and send a dense ribbon of mutated cells up the crypt while the flat mucosa has a large population of mutated cells. In addition the three effects are complementary.

These phenomenological observations are borne out by **Fig 2Eii** and **Fig 2Eiii** which show counts and percentage mutated respectively for both the crypt and the flat mucosa. These data show that the mutation causes dominance in the niche which leads to the crypt becoming entirely populated with mutated cells. This takeover of the crypt occurs faster than with just the quiescent mutation, being completed in approximately 30 days in this case (**Table 1**). The cell count data show that mutated crypts are much denser than wild type crypts associated with the neutral mutation, or arising from the simulations where the mutation affects quiescence alone.

The data also show that the flat mucosa becomes populated by approximately 95% mutated cells, which is a much higher percentage than for either the adhesion effect or quiescent effect alone. The time lag between crypt and flat mucosa infiltration was also reduced compared to previous simulations, with the exception of the adhesion-only mutation. Variability was low but consistent in the flat mucosa and very low in the crypt.

Mutation Type	Crypts with mutant cells after 1 year	Mean time to mutant population extinction (d)	Mutant dominant crypts after 1 year	Mean time to mutant domination (d)
Neutral	0	68.5	0	N/A
Adhesion	1	87.3	0	N/A
Quiescence	10	N/A	10	48.8
Apc	10	N/A	10	31.8

Table 1 Population extinctions across simulations

5. Discussion

Our results indicate that all three phenotypic alterations associated with Apc loss are selectively advantageous individually but with distinct effects. The combined Apc mutation results in a greater increase in mutated cell numbers than any of the individual mutations. A number of the results are non-intuitive and worth further examination:

- The adhesion change caused more mutated cells in the flat mucosa than in the crypt and appeared to give a small advantage in the stem cell niche
- The drag increase created very large standard deviation across the repeats and large increases in crypt cellularity
- Both quiescent time reduction and combined Apc mutation resulted in very large increases in mutated cell counts with very low standard deviations
- Apc mutation showed the separate events complementing each other

The adhesion change caused more mutated cells in the flat mucosa than in the crypt and appeared to give a small advantage in the niche – ***Fig 2B***

There appeared to be a small advantage in the niche for cells with this phenotype, as in one of the ten simulations mutated cells were still alive at the end of the simulation compared to zero in ten for the neutral mutation. Additionally, in the nine simulations where the mutated population became extinct, survival was extended compared to the case for the neutral mutation simulations. The cause of this advantage is currently unclear, as niche processes are not affected by adhesion changes. A plausible hypothesis is that mutated cells in the flat mucosa cause additional downward pressure on the side of the crypt with the mutated stem cells which would act to prevent migration out of the niche, a similar mechanism to that found by Mirams et al (18).

Adhesion favours mutated cells in the flat mucosa due to the role of anoikis, which is confined to the flat mucosa in the model in an emergent behaviour which has been explored previously (20). A cell dies whenever it loses contact with the basement membrane. As such, cells which are more tightly bound to the basement membrane will be less likely to undergo anoikis.

Additionally the flat mucosa will consist of a mix of strongly-bound mutated cells and more weakly-bound wildtype cells. In this situation the mutated cells will tend to push the wildtype cells off the basement membrane and thus can survive for much longer in the flat mucosa than normal cells.

Whilst anoikis has recently been shown to be an active process, with cells signalling neighbouring cells to push them out (21), loss of contact with the basement membrane is still required and thus increased adhesion would slow this process in the manner captured by the rules of the model used in this study.

This advantage of mutated cells in the flat mucosa may act as a previously undiscovered process for mutations becoming fixed without directly dominating via monoclonal conversion. This is apparent from the fact that the mutated cells were swept out of the crypt in nine out of the ten repeat simulations and yet survived in large numbers in the flat mucosa in all ten simulations, often long after dying out from the crypt itself. This may allow mutated cells to spread through the flat mucosa and affect neighbouring crypts.

The drag increase resulted in large increases in crypt cellularity but with large variations across repeat simulations, ***Fig 2C***

The very large standard deviation associated with the drag force effect has two key causes. The first is that cell populations with this mutation have an advantage in terms of monoclonal conversion. This is demonstrated in that three out of ten simulations have a mutated

population that never dies out, as opposed to zero out of ten in the baseline case. This advantage is likely caused by a combination of cells with this mutation effect tending to form groups due to the increased drag compared to wild-type cells, increased compression due to drag forces allowing higher cell densities than wild-type cells, and increased drag forces making it harder for mutated cells to be swept out of the crypt than wild-type cells.

The second cause of the large standard deviation of this mutation effect is that the extra compression leads to the mutant dominant crypts having more cells than wildtype dominant crypts which further amplifies the difference between simulations where mutated cells dominate and simulations where the mutated population is swept out.

Both the change in quiescent time and the combined Apc mutation had very consistent effects ***Fig 2D***
The small standard deviation in the cases of both quiescent time reduction and Apc mutation is due to the advantage that a shorter quiescent phase gives in the monoclonal conversion fight in both these cases. In both experiments the mutated populations quickly dominated the crypt in all ten simulations. This causes very little variability across the repeats.

The most striking effect of quiescent time reduction was the advantage it conferred to the mutated cells in the niche. A neutral mutation at this location was always swept out whereas a mutation resulting in a reduced quiescent phase never was. This effect causes mutated stem cells to divide fast enough to replace any cells which are swept out of the niche, while wildtype cells are not always able to replace swept out cells. This process inevitably leads to niche succession by the mutated stem cells.

Apc mutation showed the separate effects complementing each other ***Fig 2E***
The combined Apc simulation showed that the separate effects reinforced each other. One outcome of these complementary effects is the large increase in cellularity seen within the crypt. This is due to the drag effect allowing more cells to fit in a single crypt combined with the mutant dominated niche providing a constant supply of mutated cells at a higher rate than the wildtype.

Another outcome is that the flat mucosa was ultimately 95% mutated. This is due to a combination of the additional adhesion conferring an advantage to the mutated cells in the flat mucosa and the niche succession providing a ready supply of fresh mutated cells from the crypt below. This combination of effects also accounts for the reduced lag between mutated populations in the crypt and those in the flat mucosa. The adhesion advantage causes the effects of mutated cells rising up from the crypt below the mucosa to manifest much more quickly.

This work could be extended in two main directions. Firstly it would be possible to model other mutations and perform a similar analysis for them. This could take the form of either two cells with different mutations arising spontaneously in the crypt or of a single cell undergoing two successive mutations. The second direction for future work will be to model a patch of multiple crypts connected by flat mucosa. This will allow predictions to be made about the effect of a mutated crypt on a wild-type neighbour crypt and is work that we are currently undertaking.

6. Conclusions

In conclusion, a model of the colonic crypt including novel features of anoikis and accurate geometry was used to investigate the effect of Apc loss on cells within the crypt. A number of non-intuitive results arose from the simulations carried out with our extended crypt model:

- The increase in cell-membrane adhesion seen in Apc mutation allows mutated cells to live indefinitely in the flat mucosa and may be a previously unknown method of mutation fixation
- Increases in cell drag forces due to strong contact with the basement membrane confers an advantage in the monoclonal method of mutation fixation and also results in grouping of mutated cells
- Reduction in the quiescent time of mutated stem cells confers a large advantage on the mutated cells in the monoclonal method of mutation fixation

These novel predictions may prove interesting candidates for future biological and computational investigation.

7. References

1. Humphries A, Wright NA. Colonic crypt organization and tumorigenesis. Nature Reviews Cancer. 2008;8(6):415-24.
2. Cheng H, Bjerknes M, Amar J. Methods for the Determination of Epithelial-Cell Kinetic-Parameters of Human Colonic Epithelium Isolated from Surgical and Biopsy Specimens. Gastroenterology. 1984;86(1):78-85.
3. Baker A-M, Cereser B, Melton S, Fletcher AG, Rodriguez-Justo M, Tadrous PJ, et al. Quantification of Crypt and Stem Cell Evolution in the Normal and Neoplastic Human Colon. Cell Reports. 2014;8(4):940-7.
4. Bravo R, Axelrod DE. A calibrated agent-based computer model of stochastic cell dynamics in normal human colon crypts useful for in silico experiments. Theoretical Biology and Medical Modelling. 2013;10:24.
5. Cheng H, Leblond CP. Origin, Differentiation and Renewal of 4 Main Epithelial-Cell Types in Mouse Small Intestine. American Journal of Anatomy. 1974;141(4).
6. Potten CS. Stem cells in gastrointestinal epithelium: numbers, characteristics and death. Philosophical Transactions of the Royal Society B-Biological Sciences. 1998;353(1370):821-30.
7. Frisch SM, Francis H. Disruption of Epithelial Cell-Matrix Interactions induces Apoptosis. Journal of Cell Biology. 1994;124(4):619-26.
8. Hausmann M, Leucht K, Ploner C, Kiessling S, Villunger A, Becker H, et al. BCL-2 Modifying Factor (BMF) Is a Central Regulator of Anoikis in Human Intestinal Epithelial Cells. Journal of Biological Chemistry. 2011;286(30):26533-40.
9. Potten CS, Kellett M, Roberts SA, Rew DA, Wilson GD. Measurement of Invivo Proliferation in Human Colorectal Mucosa using Bromodeoxyuridine. Gut. 1992;33(1):71-8.
10. Sansom OJ, Reed KR, Hayes AJ, Ireland H, Brinkmann H, Newton IP, et al. Loss of Apc in vivo immediately perturbs Wnt signaling, differentiation, and migration. Genes & Development. 2004;18(12):1385-90.
11. Yamada S, Pokutta S, Drees F, Weis WI, Nelson WJ. Deconstructing the cadherin-catenin-actin complex. Cell. 2005;123(5):889-901.
12. Tomlinson IPM, Bodmer WF. Failure of Programmed Cell-Death and Differentiation as Causes of Tumors - Some Simple Mathematical-Models. Proceedings of the National Academy of Sciences of the United States of America. 1995;92(24):11130-4.
13. Smallbone K, Corfe BM. A mathematical model of the colon crypt capturing compositional dynamic interactions between cell types. International Journal of Experimental Pathology. 2014;95(1):1-7.
14. Murray PJ, Kang J-W, Mirams GR, Shin S-Y, Byrne HM, Maini PK, et al. Modelling Spatially Regulated beta-Catenin Dynamics and Invasion in Intestinal Crypts. Biophysical Journal. 2010;99(3):716-25.
15. Wong SY, Chiam KH, Lim CT, Matsudaira P. Computational model of cell positioning: directed and collective migration in the intestinal crypt epithelium. Journal of the Royal Society Interface. 2010;7:S351-S63.
16. Meineke FA, Potten CS, Loeffler M. Cell migration and organization in the intestinal crypt using a lattice-free model. Cell Proliferation. 2001;34(4):253-66.
17. Walker DC, Southgate J. The virtual cell-a candidate co-ordinator for 'middle-out' modelling of biological systems. Briefings in Bioinformatics. 2009;10(4):450-61.
18. Mirams GR, Fletcher AG, Maini PK, Byrne HM. A theoretical investigation of the effect of proliferation and adhesion on monoclonal conversion in the colonic crypt. Journal of Theoretical Biology. 2012;312:143-56.
19. Dunn SJ, Appleton PL, Nelson SA, Nathke IS, Gavaghan DJ, Osborne JM. A Two-Dimensional Model of the Colonic Crypt Accounting for the Role of the Basement Membrane and Pericryptal Fibroblast Sheath. Plos Computational Biology. 2012;8(5):20.

20. Ingham-Dempster T, Walker DC, Corfe BM. An agent-based model of anoikis in the colon crypt displays novel emergent behaviour consistent with biological observations. Royal Society Open Science: The Royal Society Publishing; 2017.
21. Eisenhoffer GT, Loftus PD, Yoshigi M, Otsuna H, Chien C-B, Morcos PA, et al. Crowding induces live cell extrusion to maintain homeostatic cell numbers in epithelia. Nature. 2012;484(7395):546-U183.
22. van der Wath RC, Gardiner BS, Burgess AW, Smith DW. Cell Organisation in the Colonic Crypt: A Theoretical Comparison of the Pedigree and Niche Concepts. Plos One. 2013;8(9).
23. Dunn S-J, Naethke IS, Osborne JM. Computational Models Reveal a Passive Mechanism for Cell Migration in the Crypt. Plos One. 2013;8(11).
24. Fletcher AG, Breward CJW, Chapman SJ. Mathematical modeling of monoclonal conversion in the colonic crypt. Journal of Theoretical Biology. 2012;300:118-33.
25. Pin C, Watson AJM, Carding SR. Modelling the Spatio-Temporal Cell Dynamics Reveals Novel Insights on Cell Differentiation and Proliferation in the Small Intestinal Crypt. Plos One. 2012;7(5).
26. Fellous TG, McDonald SAC, Burkert J, Humphries A, Islam S, De-Alwis NMW, et al. A Methodological Approach to Tracing Cell Lineage in Human Epithelial Tissues. Stem Cells. 2009;27(6):1410-20.

8. Acknowledgements

We would like to thank the University of Sheffield faculties of Engineering and Medicine for funding this project.

9. Figure Captions

Figure 1 The crypt. A The crypt is a structured cell factory with slow cycling stem cells at the bottom, rapidly cycling proliferative cells in the middle, and differentiated functional coloncytes at the top. Cells migrate from bottom to top. **B** Monoclonal conversion is a process whereby clonal expansion of a single stem cell eventually leads to all cells being clonal descendants of that original cell and hence carrying any mutation which existed in the original stem cell. **C** Diagram of two cells interacting with each other and the basement membrane.

Figure 2 Results. A Results of tracking a clonal population with no mechanic changes. **B** Results of increased cell-extracellular matrix adhesion. **C** Results of increased drag due to increased membrane adhesion. **D** Results of reducing stem cell quiescent time. **E** Results of overall Apc Mutation. In all figures: i) Visualistion from simulation with this mutation. ii) Absolute counts of mutated cells in crypt and flat mucosa over ten repeats. iii) Percentages of cells mutated in crypt and cells mutated in flat mucosa over ten repeats.

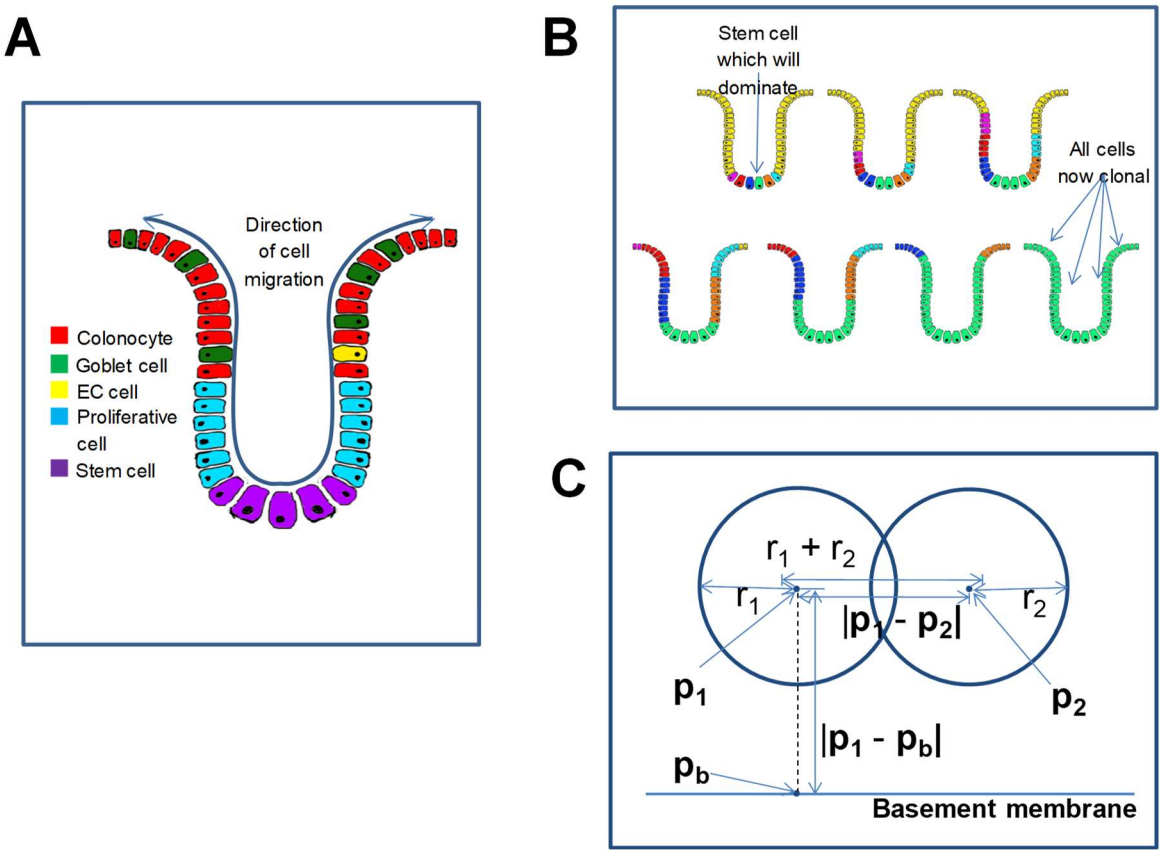
A
Direction
of cell
migration
Colonocyte
Goblet cell
EC cell
Proliferative
cell
Stem cell
B
Stem cell
which will
dominate
All cells
now clonal
C
r1 + r2
r1
r2
|p1 - p2|
p1
p2
|p1 - pb|
pb
Basement membrane

Figure 1

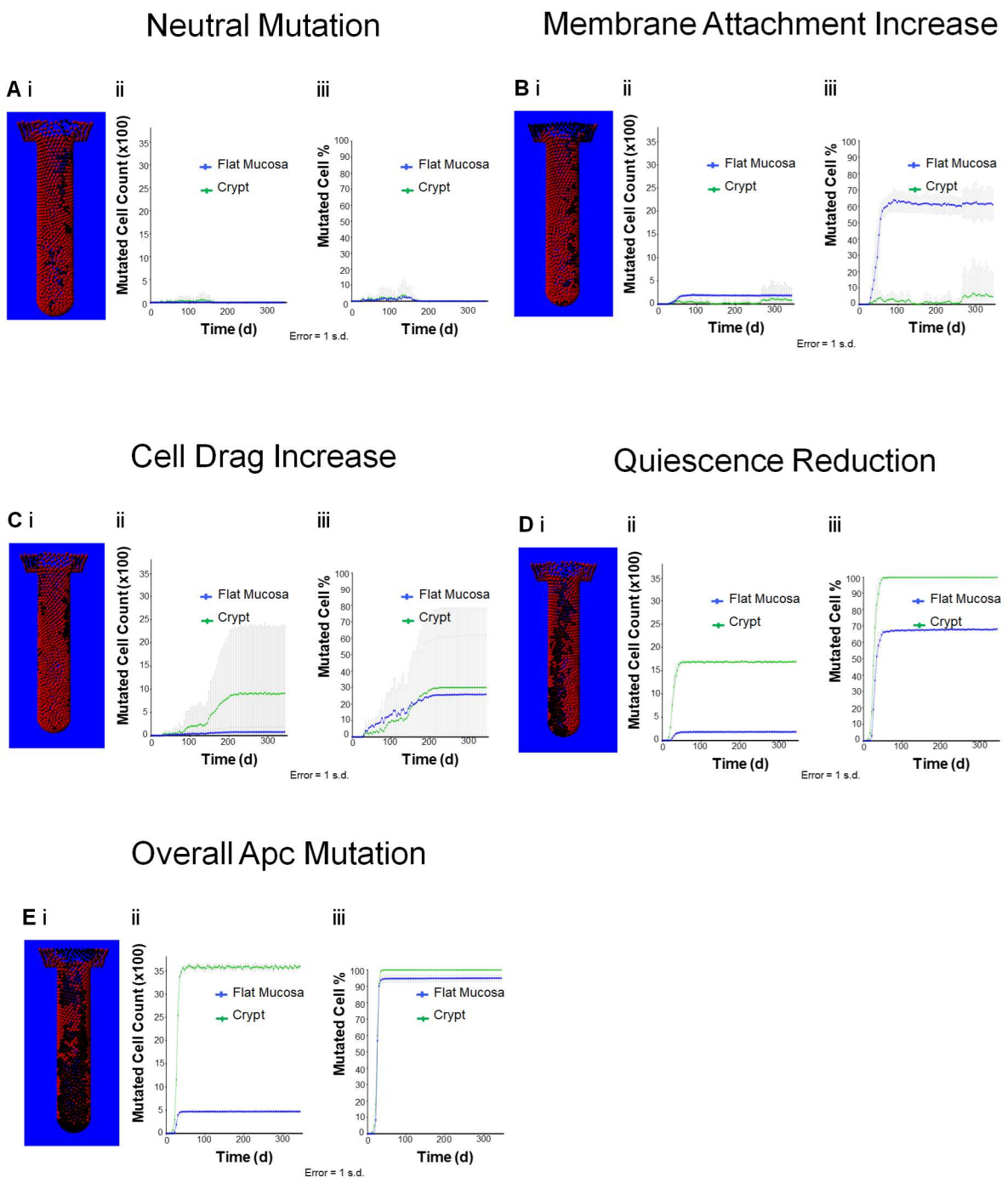
Neutral Mutation
Membrane Attachment Increase
A i
ii
iii
B i
ii
iii
Mutated Cell Count (x100)
Mutated Cell %
Flat Mucosa
Crypt
Time (d)
Error = 1 s.d.
Cell Drag Increase
Quiescence Reduction
C i
ii
iii
D i
ii
iii
Overall Apc Mutation
E i
ii
iii

Figure 2